

Structural, textural and acid-base properties of carbonates-containing hydroxyapatites

Lishil Silvester^{a,b}, Jean-François Lamonier^{a,b}, Rose-Noëlle Vannier^{a,b,c}, Carole Lamonier^{a,b}, Mickaël Capron^{a,b}, Anne-Sophie Mamede^{a,b,c}, Frédérique Pourpoint^{a,b,c}, Antonella Gervasini^d and Franck Dumeignil^{a,b,e*}

Supplementary information

10

15

20

25

30

35

40

45

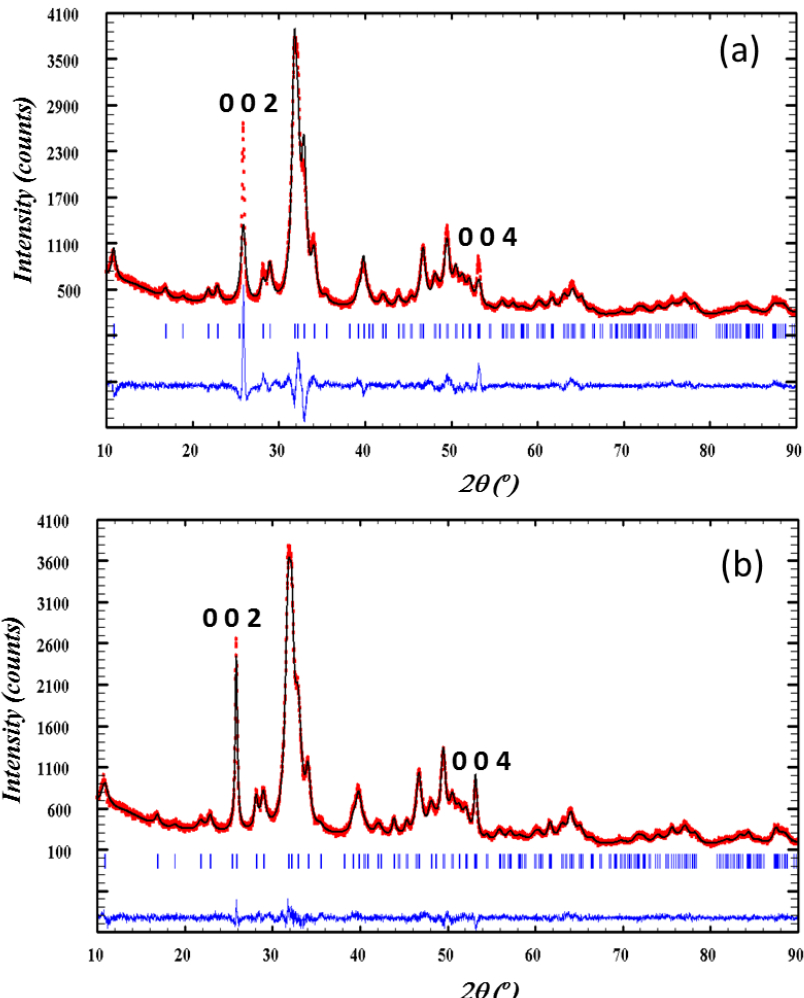


Fig.S1 Calculated X-ray diffraction profiles of Hap D (black lines) compared to experimental data (red dots) showing a poor agreement between calculated and experimental profiles for 002 and 004 Bragg peaks when an isotropic size-broadening model is used (a) and a good agreement when an anisotropic size-broadening model is used (b).

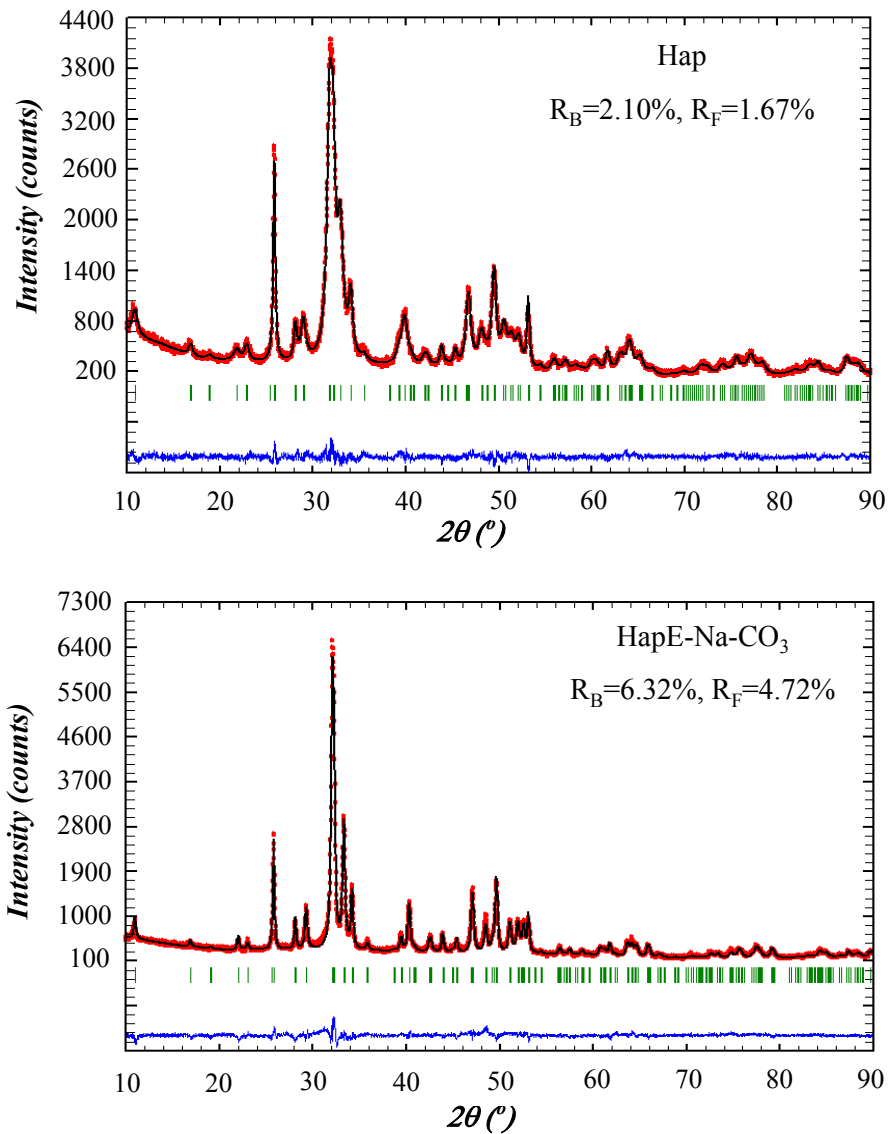


Fig.S2 Calculated X-ray diffraction profiles of Hap and HapE-Na-CO₃ samples (black lines) compared to experimental data (red dots) showing a good agreement between calculated and experimental profiles as shown by the difference in blue. R_B and R_F , the reliability factors, are given to attest the quality of the structure model.

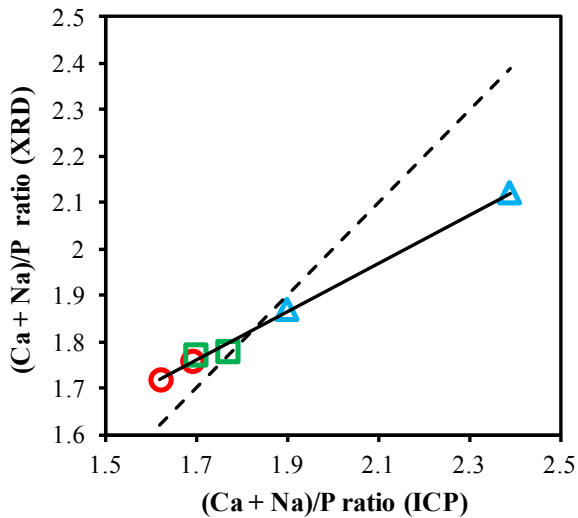
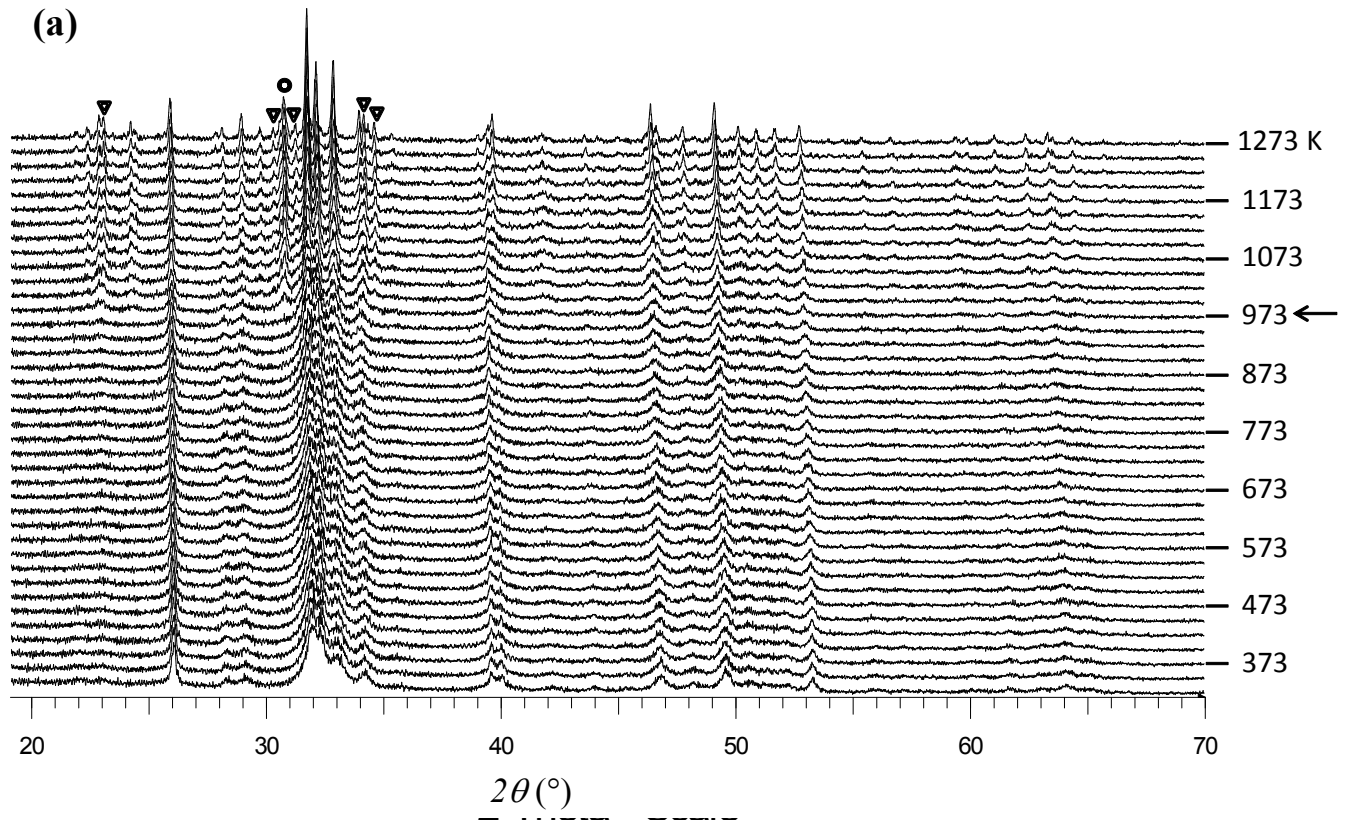


Fig.S3 (Ca + Na)/P ratio calculated from XRD refinement as a function of the ICP (Ca + Na)/P ratio (circles representing HapD and Hap, squares for carbonated apatites, namely Hap-CO₃ and HapNa-CO₃, and triangles for carbonate-rich apatites, namely HapE-CO₃ and HapE-Na-CO₃). The dashed line represents the theoretical perfect correlation (1 to 1).

5



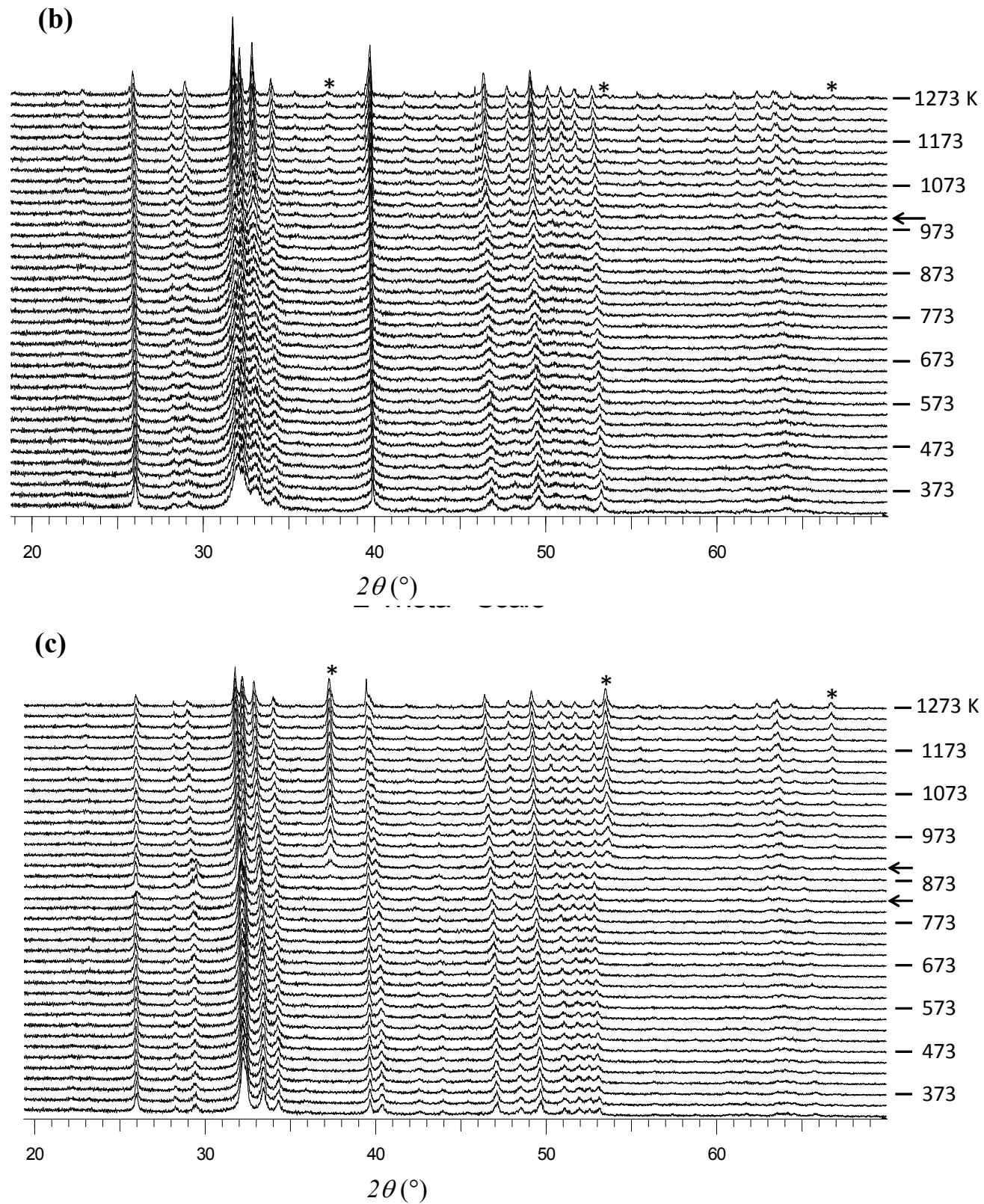


Fig.S4 XRD patterns of (a) HapD [arrow pointing the temperature for the appearance of $\text{Ca}_3(\text{PO}_4)_2$ phases mainly at $2\theta = 30^\circ$ & 34.5°], (b) Hap-CO₃ [arrow representing the formation of CaO phase at $2\theta = 37^\circ$] and (c) HapE-Na-CO₃ [arrow at 823 K showing the reconstruction of apatite structure and the formation of CaO phase for $2\theta = 37^\circ$, 53.5° & 66.5° at 898 K] collected during temperature increase under air.

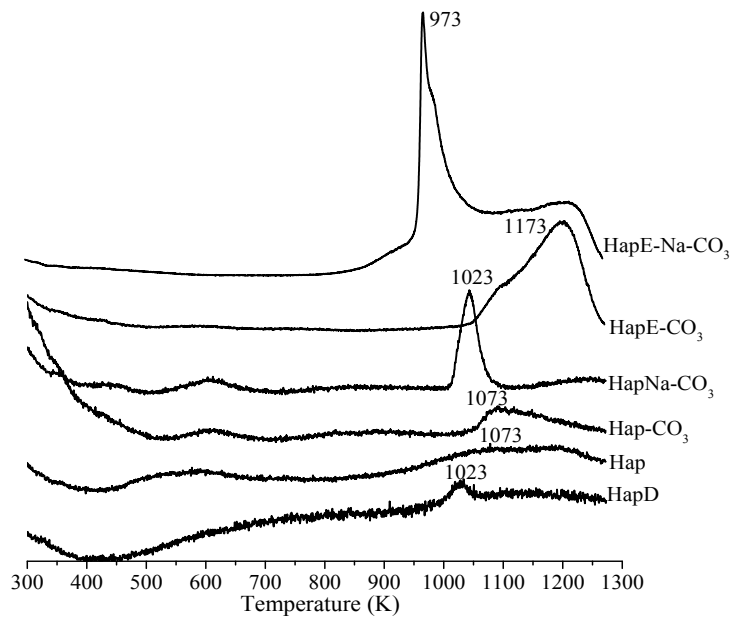


Fig. S5 Derived TGA curves of apatite solids obtained using MS with $m/z = 44$ showing the CO_2 loss.

5

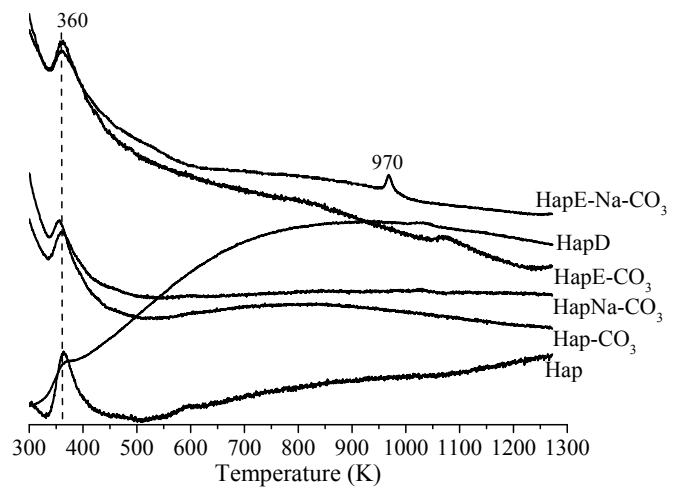


Fig. S6 Derived TGA curves of apatite solids obtained using MS with $m/z = 18$ showing the H_2O loss.

10

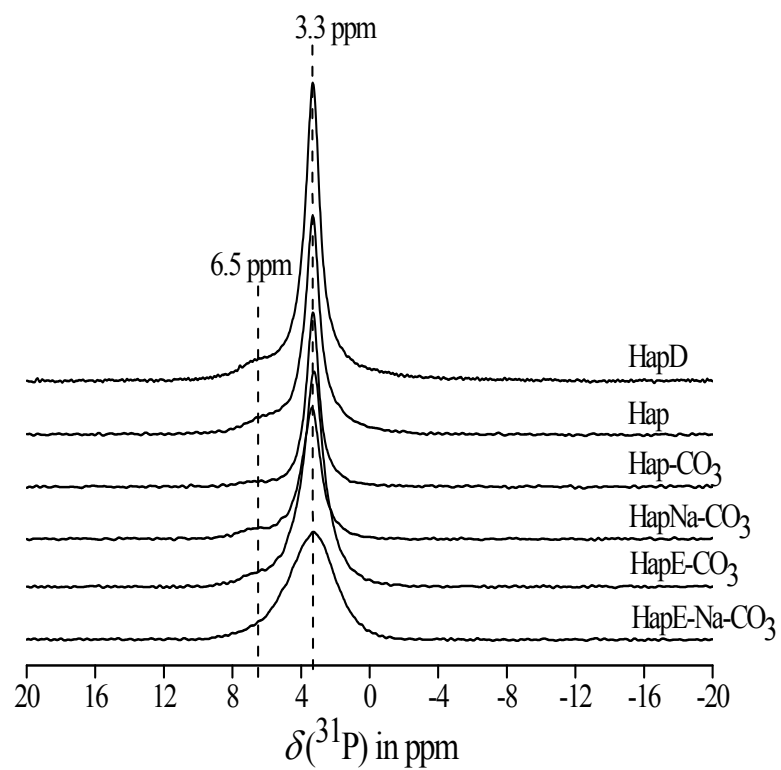


Fig. S7 ^{31}P CP MAS-NMR spectra of the hydroxyapatite solids.

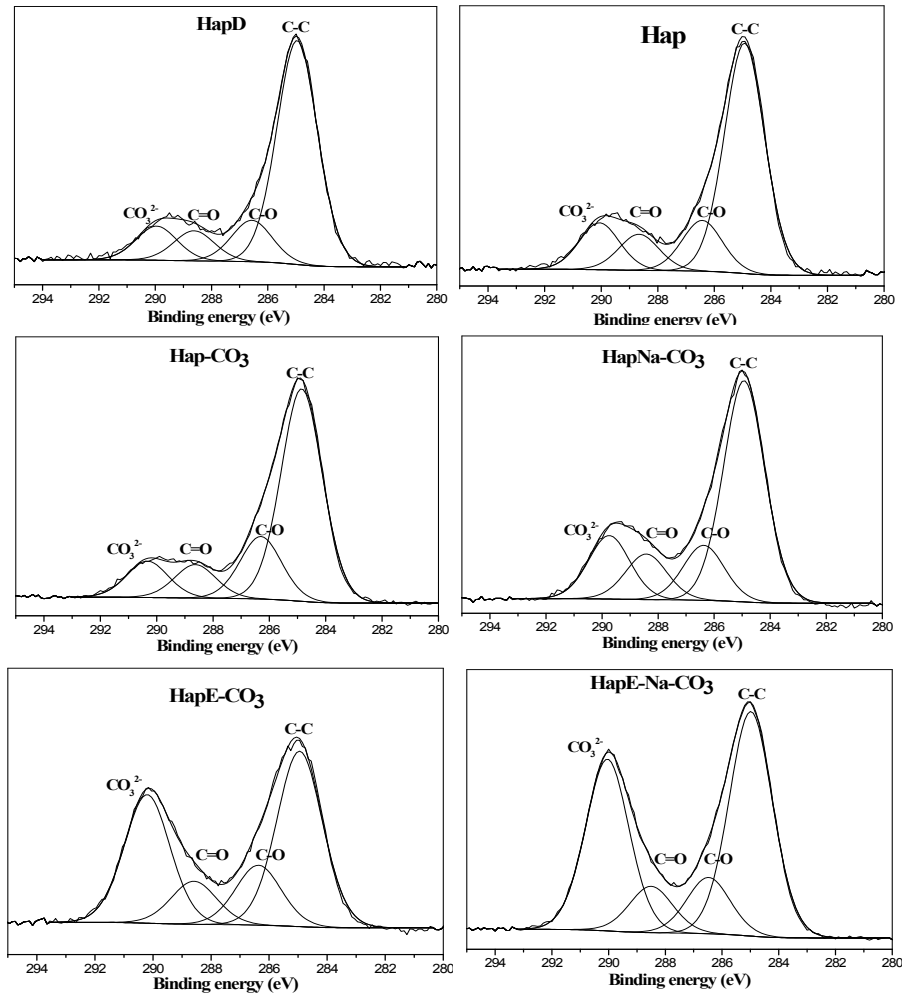


Fig.S8 C1s photopeak of the samples.

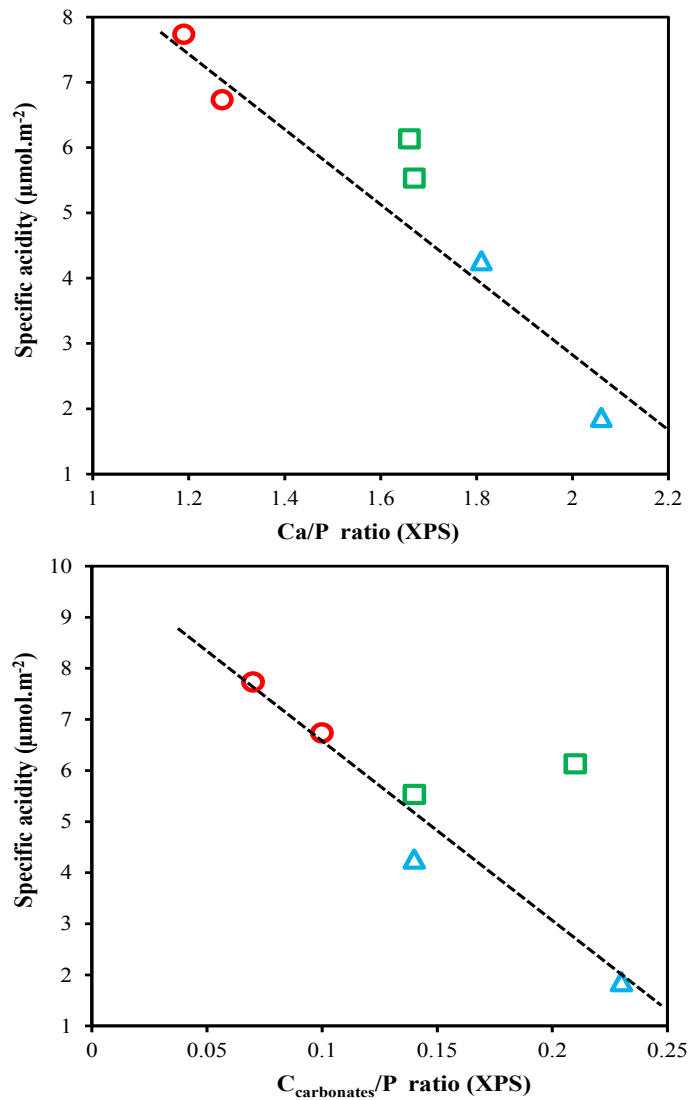


Fig.S9 Specific acidity of the solids as a function of the surface Ca/P and the C_{carbonates}/P ratios (circles representing HapD and Hap, squares for carbonated apatites, namely Hap-CO₃ and HapNa-CO₃, and triangles for carbonate-rich apatites, namely HapE-CO₃ and HapE-Na-CO₃).